Electronic Supplementary Material (ESI) for RSC Advances.

Performance of hybrid nanostructured conductive cotton threads as LPG sensor at ambient temperature: Preparation and analysis

N.G. Shimpi*[2], D.P. Hansora[1], R. Yadav[1], S. Mishra[1]

[1]University Institute of Chemical Technology, North Maharashtra University, Jalgaon-425001

[2]Department of Chemistry, University of Mumbai, Kalina, Santacruz East, Mumbai-400098 Maharashtra, India

***Corresponding Author:**

Dr. Navinchandra Shimpi, Phone No: +91-22-26543575

Email ID: navin_shimpi@rediffmail.com

Supplementary Information:

S1. Motivation from previous work

CNT is an intriguing form of pure carbon sheet, which is Iijima's (et al 1991) a new era of innovative research. CNT is clinographic perspective of conceivable structure of graphitic tubule [1]. Single wall carbon nanotubes (SWCNTs) and multi wall carbon nanotubes (MWCNTs) are the two types of CNTs. Methods employed for their synthesis are arc-discharge, laser ablation and chemical vapor deposition (CVD) method [2-6]. Among these methods, CVD is advantageous for large scale production in which catalyst disintegrates the hydrocarbon atoms and the role of catalysts determines the type, morphology, diameter and growth mechanism of CNTs [3,6-8]. Based on various gas sensing methods, sensing technology has become more significant because of its widespread and common applications [9-10].

Semiconducting metal oxides, membranes and solid electrolytes have been researched, which show their sensing capability [11]. Semiconducting materials like SnO_2-αFe_2O_3 multilayers [9], $WO_{2.72}$ nanowires [12] and α-Fe_2O_3 nanotubes have been used as H_2S sensors [13]. Chemiresistive sensors (SWCNTs covalently functionalized with urea, thiourea, and squaramide) arrays have demonstrated a long-term stability and suitability for detection of explosive materials like cyclohexanone and nitro methane [14-15].

A phenomenon of intrinsically conducting polymers (CPs) based gas sensor is predominantly focused around the sensation because of their change in electrical conductivity upon exposure of analyte vapors [16-19]. Moreover, the strategical synthesized ternary CNT/PAni composites consolidated by noble metal nanoparticles, metal oxide, or graphene sheets are conceivably found suitable in applications of chemical sensors, fuel cells, electronic devices and capacitors [20]. Nanostructured composites of PMMA/carbon have been used for detecting vapors of acetone, methanol, ethanol [21]. Blend of two nanomaterials *i.e.*, PAni incorporated

using CNT hybrid nanomaterials [22] and PAni-ZnO nanocomposites [23-24] were used as sensors to detect vapors of ammonia. A p-PAni/n-TiO_2 heterojunction based sensor can give maximum response of 63 % upon exposure to 0.1 vol % LPG at room temperature [25]. The bio sensors based on CNT/polymer composites have been found for quantitative and qualitative analysis of DNA, enzymes, proteins, antigens and metabolites [26]. Various polymers like poly(ethylene oxide) (PEO) and poly(vinyl alcohol) (PVA) were decorated using CNTs, and hence resulting polymer nanocomposites can be useful sensors for detection of organic vapours like methanol, ethanol, isopropyl alcohol, chloroform and water [27-28].

On other hand, linear shaped electrode materials like cotton strings, threads, fibres and yarns appear to be the most commonly preferred materials for development of cable-type wearable sensing gadget. These linear materials are versatile, adaptable, flexible and permeable, which are generally composed of multiple individual weaving cotton fibrils bundled together. In this regard, porous cotton threads can be made profoundly conductive using basic submersion of a CNT without affecting its shape, because CNTs have solid Van der Waals interactions with this sort of poly-D glucose chains based micro fibrils. After the adsorption of CNTs, threads are allowed to dry out, which make difficult to expel the adsorbed CNTs from the surface of threads by exposure to solvents, heat, or a combination of both. Such a hierarchical network creates a confounded and highly porous morphology, which meets the necessities of immaculate wearable sensing technology [29-30]. These permeable conductive textiles have been receiving a much interest for smart wearable devices.

REFERENCES

1. S. Iijima, *Lett. Nat.,* 1991, **354**, 56-58. http://dx.doi.org/10.1038/354056a0
2. H. Dai, *Surf. Sci.,* 2002, **500**, 218-241. http://dx.doi.org/10.1016/S0039-6028(01)01558-8

3. V.N. Popov, *Mater. Sci. Eng. R,* 2004, **43**, 61-102. http://dx.doi.org/10.1016/j.mser.2003.10.001
4. C.E. Baddour and C. Briens, *Int. J. Chem. React. Eng.,* 2005, **3**, 20-22. http://dx.doi.org/10.2202/1542-6580.1279
5. K. Matzinger, *Ph.D. Theses*, Universität Freiburg, 2006. https://doc.rero.ch/record/6666/files/MatzingerK.pdf
6. N.G. Shimpi, S. Mishra, D.P. Hansora and U. Savdekar, *Indian Pat.*, 3179/MUM/2013, 2013. http://ipindia.nic.in/ipr/patent/journal_archieve/journal_2013/pat_arch_102013/official_journal_25102013_part_i.pdf
7. H. Cui, G. Eres, J.Y. Hawe, A. Puretkzy, M. Varela, D.B. Geohegan and D.H. Lowndes, *Chem. Phys. Lett.,* 2003, **374**, 222-228. http://dx.doi.org/10.1016/S0009-2614(03)00701-2
8. N. Gupta, S. Sharma, I.A. Mir and D. Kumar, *J. Sci. Ind. Res.,* 2006, **65**, 549-557. http://nopr.niscair.res.in/bitstream/123456789/4862/1/JSIR%2065(7)%20549-557.pdf
9. G. Sberveglieri, *Sens. Actuators, B* 1995, **23**, 103-109. http://dx.doi.org/10.1016/0925-4005(94)01278-P
10. X. Liu, S. Cheng, H. Liu, S. Hu, D. Zhang and H. Ning, *Sens.,* 2012, **12**, 9635-9665. http://dx.doi.org/10.3390/s120709635
11. B. Adhikari, S. Majumdar, *Prog. Polym. Sci.,* 2004, **29**, 699-766. http://dx.doi.org/10.1016/j.progpolymsci.2004.03.002
12. C.S. Rout and M. Hegde, C.N.R. Rao, *Sens. Actuators, B,* 2008, **128**, 488-493. http://dx.doi.org/10.1016/j.snb.2007.07.013
13. Z. Sun, H. Yuan, Z. Liu, B. Han and X. Zhang, *Adv. Mater.,* 2005, **17**, 2993-2997. http://dx.doi.org/10.1002/adma.200501562

14. T. Zhang, S. Mubeen, N.V. Myung and M.A. Deshusses, *Nanotechnol.,* 2008, **19**, 1-14. http://dx.doi.org/10.1088/0957-4484/19/33/332001

15. J.M. Schnorr, D.V. Zwaag, J.J. Walish, Y. Weizmann and T.M. Swager*, Adv. Funct. Mater.,* 2013, **23**, 5285-5291. http://dx.doi.org/10.1002/adfm.201300131

16. K.C. Persaud, *Mater. Today,* 2005, **8**, 38-44. http://dx.doi.org/10.1016/S1369-7021(05)00793-5

17. J. Janata and M. Josowicz, *Nat. Mater.,* 2003, **2**, 19-24. http://dx.doi.org/10.1038/nmat768

18. B. Yeole, T. Sen, D.P. Hansora and S. Mishra. *J. Appl. Polym. Sci.,* 2015*,* **132**, 1-9. http://dx.doi.org/10.1002/app.42379

19. S. Mishra, N.G. Shimpi and T. Sen, *J. Polym. Res.,* 2013*,* **20**, 49. http://dx.doi.org/10.1007/s10965-012-0049-5

20. C. Oueiny, S. Berlioz and F.X. Perrin, *Prog. Polym. Sci.,* 2014, **39**, 707-748. http://dx.doi.org/10.1016/j.progpolymsci.2013.08.009

21. L. Quercia, F. Loffredo, M. Bombace, A.D. Girolamo, D. Mauro and G.D. Francia, Proceeding of an International Conference on the Eurosensors, Italy, 2005. http://www.afs.enea.it/devito/Abstract_Eurosensors/ExtabsEUS05Comp.pdf

22. M. Ding, Hybrid materials based on carbon nanotubes and graphene: synthesis, interfacial processes, and applications in chemical sensing, *Ph.D. Theses,* University of Pittsburgh, 2013. http://d-scholarship.pitt.edu/19257/4/Mengning_Ding_ETD_2013.pdf

23. L.A. Patil, M.D. Shinde, A.R. Bari, V.V. Deo, D.M. Patil and M.P. Kaushik, *Sens. Actuators B,* 2011, **155**, 174-182. http://dx.doi.org/10.1016/j.snb.2010.11.043

24. S.L. Patil, M.A. Chougule, S. Sen and V.B. Patil, *Meas.,* 2012, **45,** 243-249. http://dx.doi.org/10.1016/j.measurement.2011.12.012

25. D.S. Dhawale, R.R. Salunkhe, U.M. Patil, K.V. Gurav, A.M. More and C.D. Lokhande, *Sens. Actuators, B,* 2008, **134**, 988-992. http://dx.doi.org/10.1016/j.snb.2008.07.003

26. H.J. Salavagione, A.M. Diez-Pascual, E. Lazaro, S. Vera and M.A. Gomez-Fatoua, *J. Mater. Chem. A,* 2014, **2**, 14289-14328. http://dx.doi.org/10.1039/c4ta02159b

27. V.K. Rana, S. Akhtar, S. Chatterjee, S. Mishra, R.P. Singh and C.S. Ha, *J. Nanosci. Nanotechnol.,* 2014, **14**, 2425-2435. http://dx.doi.org/10.1166/jnn.2014.8498

28. P.M. Abbasi and S.R. Ghaffarian, *RSC Adv.,* 2014, **4**, 30906-30913. http://dx.doi.org/10.1039/C4RA04197F

29. B.S. Shim, W. Chen, C. Doty, C. Xu and N.A. Kotov, *Nano Lett.,* 2008, **8**, 4151-4157. http://dx.doi.org/10.1021/nl801495p

30. B.S. Shim, *Ph.D. Theses*, The University of Michigan, 2009. http://deepblue.lib.umich.edu/bitstream/handle/2027.42/62251/bshim_1.pdf?sequence=1

S2. Synthesis of catalyst nanoparticles

Detail steps involved in preparation of Fe/MgO catalyst nanoparticles (K1, K2 and K3) are discussed as per following, while Figure S1 shows its schematic.

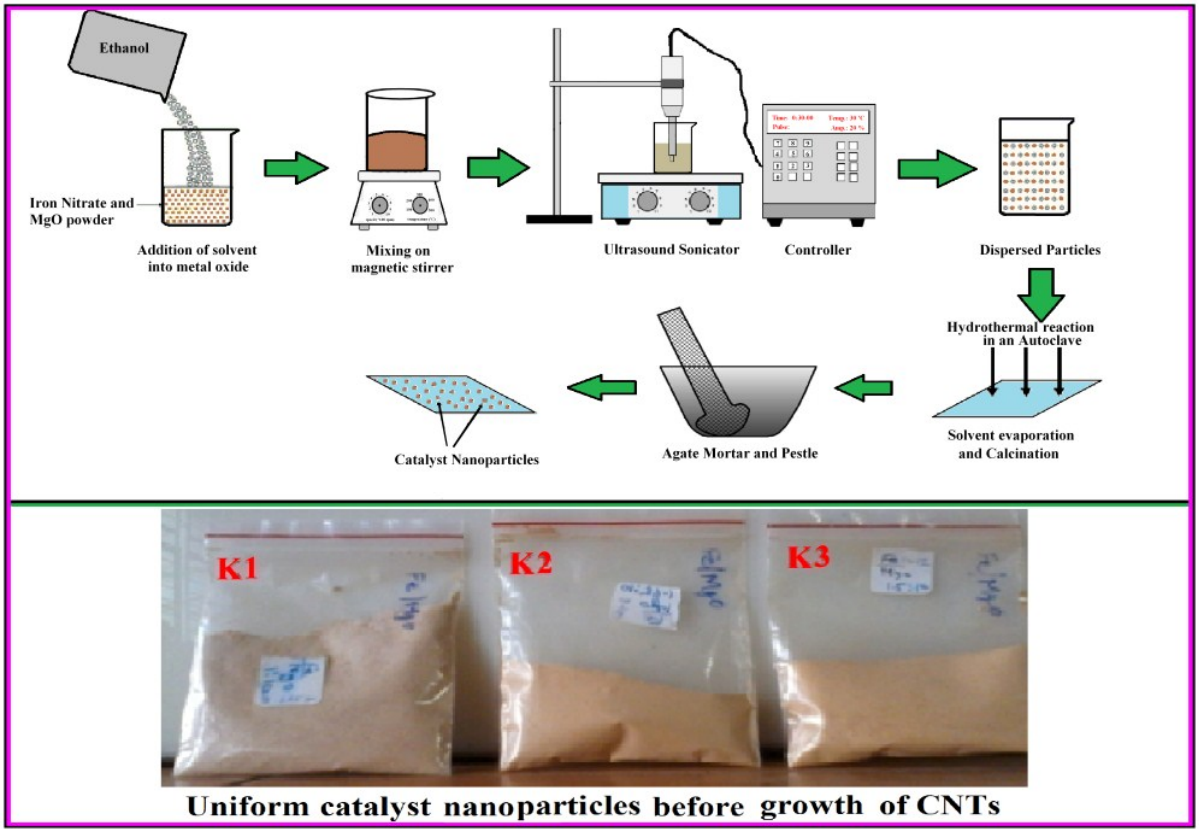

Figure S1. Process steps for preparation of catalyst (Fe/MgO) nanoparticles

A stoichiometric amount of reactants were taken in ethanol as solvent. A ratio of Fe to MgO was varied from 0.1 to 0.15 wt %. Predetermined amount of iron nitrate [$Fe(NO_3)_3 \cdot 9H_2O$] and MgO solutions were blended together under controlled and continuous stirring for 60 min by using magnetic stirrer (Remi Elektro technik limited, Mumbai, India). Further this blend was ultrasonicated (BO3 Ultrasonic Processor UP 1200, Cromtech, India) for 30 min at pulse rate of 5 sec for on/off. The MgO was supported over $Fe(NO_3)_3 \cdot 9H_2O$, which was adhered and balanced using hydrothermal treatment using autoclave reactor (Amar Equipments Private Limited, Mumbai, India). The process parameters of autoclave reactor were set as

temperature of 150 ^{o}C and pressure of 60 psi for the duration of 120 min. The resulted precipitates were filtered using nylon filter (60 mesh) and then kept in muffle furnace (Bio Technics, Mumbai, India) for aging at 500 ^{o}C for 20 min. The product was crushed in mortar pastel which resulted fine powder. These catalyst nanoparticles were used for CNT growth by CVD method.

S3. Construction design and working of CVD reactor

For preparation of CNTs, CVD reactor set up was designed and purchased from Lelesil Innovative System, Mumbai, India. This set up is consisted of horizontal quartz glass tube, heating furnace as barrel and heating control system. Table S1(a-c) shows the details of its dimensions. The safe operating procedure was followed to run the CVD reactor set up.

Table S1(a). Dimensions of horizontal reactor glass tube

Sr. No.	**Component of tube**	**Detail/dimension**
1.	OD	45 mm +/- 1mm
2.	ID	40 mm +/- 1mm
3.	Length	1280 mm +/- 1mm end to end
4.	Material of construction	Quartz

Table S1(b). Dimensions of furnace structure

Sr. No.	**Component of furnace**	**Detail/dimension**
1.	Length	1000 mm +/- 10 mm
2.	ID of tube	50 mm +/- 1 mm
3.	OD of tube	55 mm +/- 1 mm
4.	Operating temperature	1000 ^{o}C
5.	Material of Hollow tube	High temperature moulded ceramic
6.	Material of construction	Heavy 2mm metal fab sheets square shape
7.	Support structure	4 Pole for table top mounting
8.	Type of design	Three zone heating type horizontal tubular furnace

Table S1(c). Dimensions of heating system

Sr. No.	Component of heating system	Detail/dimension
1.	Power control	Single phase with through the phase angle controlled drive
2.	Heating elements	Designed to with stand heat up to 1100 °C
3.	Type of element	Solid type / Coil type Kanthal A1 heating element
4.	Total length of element	1000 mm +/– 10mm
5.	Resistance of the element	1.24 ohms
6.	Working temperature	1000 °C (for continuous operation) 3 hours
7.	Power	10 kW line load
8.	Electrical line details	40 Amp – MCB single phase with neutral
9.	Power cable	4 Core armoured cable with wire 2m each

A furnace was placed at horizontal position on a platform under control balance. The furnace has three partitions of heating zones (Figure S2). The stainless steel braded sensors were provided at back side of furnace. The connectors were attached to each zone along with temperature indicators. Each zone was connected with temperature probes. The heating control system can be powered and controlled on using the temperature controller.

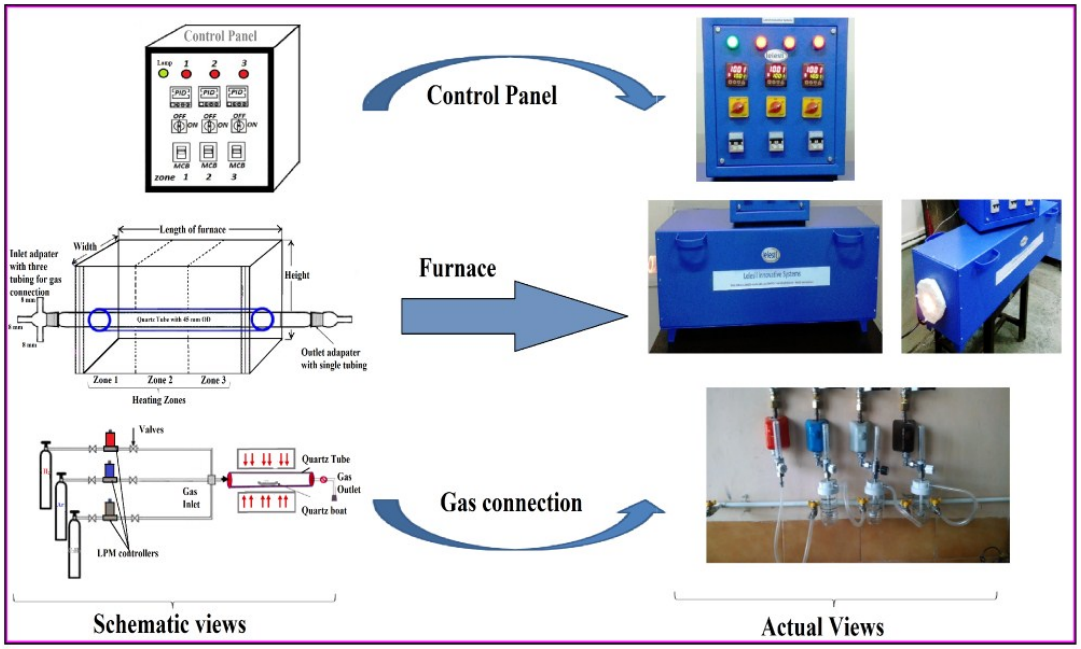

Figure S2. Schematic v/s actual views of CVD setup

The indicators provided on the system were numbered as 1, 2 and 3 for each three zones, which are also shown in schematic of Figure S2. The yellow rotary switches were provided to each zone for on/off service. A furnace was capable to withstand temperature up to 1000 ^{o}C, which can be also seen in Figure S2 indicating the temperature range of 0-1000 ^{o}C in PID display. Once the heating was started the central zone was get heated rapidly as compared to zone 1 and 3. Quartz tube (outer diameter of 45 mm with reduced diameter of 40 mm at the both ends) was designed with provision of placing a 30 mm quartz boat which was capable to carry catalyst nanoparticles in it. Once the quartz boat was placed, both inlet and outlet adopters were connected at both ends of quartz tube with grease over the surface. Both adapters were tightened using metal springs to avoid leakages. Inlet adapter was designed in such a way that three different gaseous can be supplied from three points, while outlet adaptor was facitilized with one point for removal of gaseous impurities.

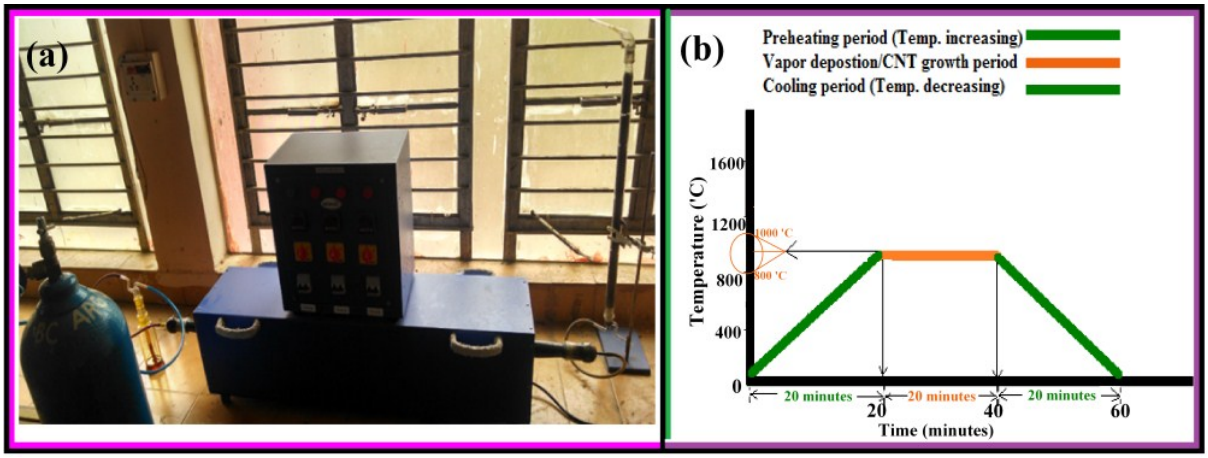

Figure S3. (a) Arrangement of CVD reactor setup in laboratory and (b) Graphical process steps illustrating synthesis of CNTs by CVD method

Figure S3(a) illustrates arrangement of CVD reactor set up in the laboratory, while Figure S3(b) shows graphical presentation of steps involved in synthesis of CNTs by CVD method using carbon precursors.

S4. Synthesis of CNTs by CVD method

Predetermined amount (0.5 gm) of catalyst nanoparticles was uniformly distributed in a quartz boat and placed at the centre of the quartz tube of a CVD reactor set up. Argon gas was purged with flow rate of 50 mL for 15 minutes. Meanwhile, the furnace was heated at set temperature (900 ^{o}C). Once the set temperature was attained, xylene was allowed to vaporise with argon (carrier) gas for predetermined residential time. Growth of CNTs was observed after stipulated time, the flow of gas mixture was stopped and heating system was switched off. A furnace was cooled down to 30 ^{o}C temperature by flowing argon gas. The boat was discharged from the furnace and samples were collected.

S5. Strategical steps for purification of CNTs

The sample was also subjected to liquid-phase oxidation using 10% HNO_3 solution. During this step, amorphous carbon was removed without damaging the tube walls, since the physical properties of the tubes could change if defects are present. CNTs were sonicated in 10% HNO_3 solution at 50 ^{o}C for 30 min to decontaminate and simultaneously exfoliate the bundles. In acid treatment step, 200 mg of oxidized CNTs was added in 35% HCl and allowed to sonicate for 30 min which removed the influence of MgO support. The elimination of catalyst from the samples was partially accomplished by acid treatment with 10% HNO_3 at an ambient temperature. However, it is worth noting that the acid treatment was unable to remove all the catalytic particles. The acid treatment at room temperature demonstrated ineffectual in eliminating all the metallic particles, mainly those enclosed in carbon confines or shells. However, it was found that when acid extracted the metallic core of these protected particles, their carbon nanostructures remained such as. It was difficult to oxidize protected metallic particles, carbon nanostructures without significantly damaging CNTs. Therefore, last chemical step of the cleansing strategy was a mild water treatment. In

last step of the purification, the CNTs were dispersed in DM water by sonication. This dispersion was allowed to settle, after which the supernatant phase was separated and filtered. The supernatant liquid was decanted in ultra-centrifuge (C-30 BL, Remi Elektrotechnik limited, Mumbai, India). The residual solid was washed repeatedly using DM water and allowed to centrifuge again. The CNTs were neutralized with DM water and trapped on a filter paper. These filtered CNTs were dried in an oven (Bio Technics, Mumbai, India) at 100 ^{o}C for 48 hr. The obtained dry CNT was in the pure form.

S6. Construction of gas sensing set up

A ‘static gas sensing setup’ was used, in which electrical feeds were attached through the base plate. The current passing through the heating element was monitored using a relay operated with an electronic circuit having adjustable ON–OFF knob. A gas inlet valve was fitted at one of the ports provided at the top plate. Inlet valve was provided to inject predetermined volume of gas inside the static system (Figure S4) using an injection syringe. Digital picoammeter was attached to sensing set up, which was used to measure current when constant voltage was applied.

Figure S4. Photographic representation of a two-probe gas sensing setup at laboratory

S7. Growth of CNTs

Growth of CNTs was observed at different temperatures ranging from 500 to 1000 ^{o}C. Figure S5 shows SEM and TEM cross-section micrographs of CNTs growth over K3 catalyst after 20 min. CNTs were not observed on the substrate at 500-900 ^{o}C. The growth was observed at >600 ^{o}C with the majority presence of MWCNTs which were aligned vertically as shown in Figure S5(a-d). Further increment in temperature (up to 900 ^{o}C) may decrease the length of CNTs without vertical alignment. This is because of decrement in density and absence of crowding. Their length was estimated to be about 100-200 nm, which can be observed from Figure S5(a-d). FE-SEM micrograph in Figure S5(e) shows aligned MWCNTs dramatically reached a length of about less than 1 μm.

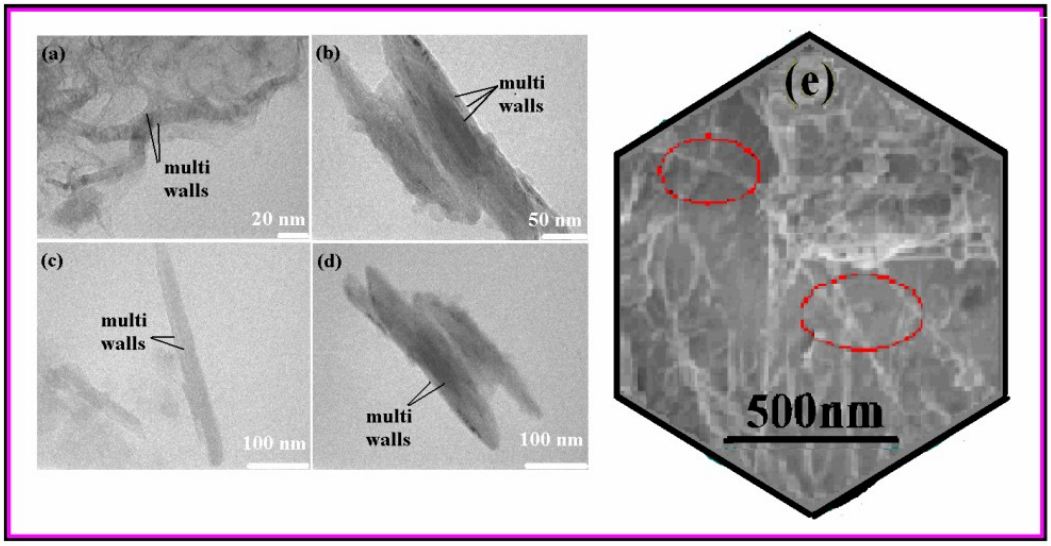

Figure S5. (a-d) TEM micrographs of CNTs showing growth, (e) FE-SEM micrographs of CNTs

More CNT bundles can be observed at > 900 ^{o}C, while Figure S5(e) demonstrates that MWCNTs having small diameters might be exist at 1000 ^{o}C or even SWCNTs. It should be noted that these CNTs bundles are emerged from different growth sites. Furthermore, some CNTs were also found to be separated from a bundle after its formation and it was

incorporated into another bundle nearby, producing CNT networks. Bundles having large diameters can be observed clearly to extend upward from the surface, and others appeared close nearer to the substrate with random direction. Both the CNT diameter and nucleation density were reduced at 1000 ^{o}C, which can be revealed from Figure S5(e). The images reveal that the surface of each catalyst nanoparticles is completely covered by large amounts of pure CNTs. But after purification, these CNTs are oriented uniformly without any visible defects. In general, the size distribution of the CNTs is determined by the catalyst nanoparticles, and CNTs can only grow on catalyst nanoparticles and have almost smaller diameter as similar to catalyst nanoparticles.

S8. Thermo gravimetric analysis (TGA)

The TGA analysis of CNTs, PAni/γ-Fe_2O_3 nanostructures and CNT/PAni/γ-Fe_2O_3 hybrid nanocomposite was performed on a thermo gravimetric analyzer (TGA 50, Shimadzu, Tokyo, Japan) over a temperature range of 30-850 ^{o}C with heating rate of 10 ^{o}C/min. The TGA analysis was done under inert atmosphere by keeping nitrogen gas flow rate of 850 mL/min.

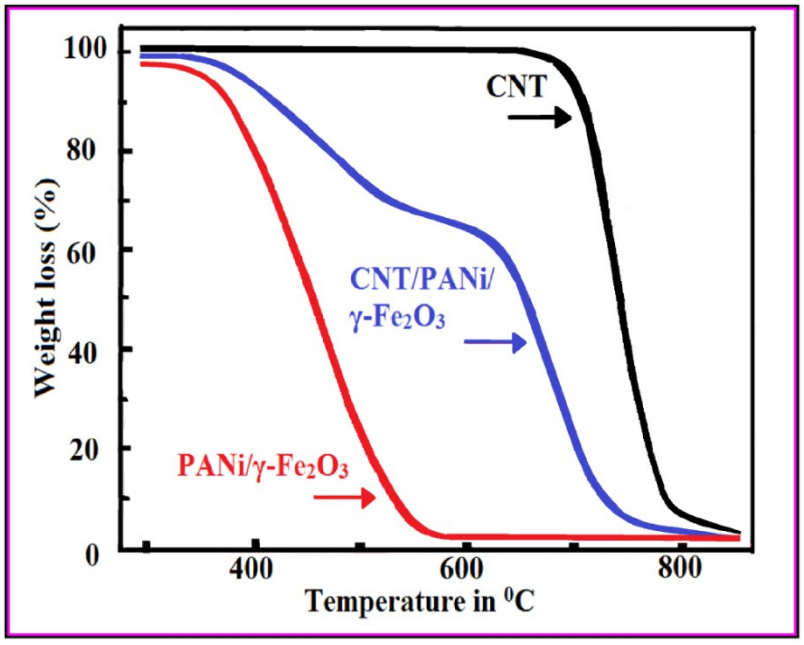

Figure S6: Thermographs of CNT, PANi/γ-Fe_2O_3 and CNT/PANi/γ-Fe_2O_3 nanostructures

Figure S6 illustrates thermal behavior of CNTs, PAni/γ-Fe_2O_3 nanocomposites and CNT/PAni/γ-Fe_2O_3 nanostructures. The decomposition temperature of CNT, PAni/γ-Fe_2O_3 nanocomposites and CNT/PAni/γ-Fe_2O_3 hybrid nanostructures were observed as 700, 530 and 390 ^oC, respectively. This shows that hybrid nanostructures were thermally stable due to uniform shifting of heat and presence of CNTs. Moreover, CNT itself is a more stable.